Multiple attractors and global bifurcations in a Kaldor-type business cycle model[*]

Gian Italo Bischi[1], Roberto Dieci[2], Giorgio Rodano[3], and Enrico Saltari[1]

[1] Istituto di Scienze Economiche, University of Urbino, 61029 Urbino, Italy
   (e-mail: bischi@econ.uniurb.it; esaltari@microelettra.it)
[2] Dipartimento di Economia, University of Parma, via Kennedy 6B, 43100 Parma, Italy
   (e-mail: roberto.dieci@unipr.it)
[3] Dipartimento di Teoria Economica e Metodi Quantitativi, Università "La Sapienza", Roma, Italy
   (e-mail: g.rodano@dte.uniroma1.it)

Abstract. We consider a Kaldor-type discrete-time nonlinear business cycle model in income and capital, where investment is assumed to depend both on the difference between normal and current levels of capital stock, and on the difference between the current income and its normal level, through a nonlinear S-shaped increasing function. As usual in Kaldor business cycle models, one or three steady states exist, and the standard analysis of the local stability and bifurcations suggests that endogenous oscillations occur in the presence of only one unstable equilibrium, whereas the coexistence of three equilibria is characterized by bi-stability, the central equilibrium being on the boundary which separates the basins of the two stable ones. However, a deeper analysis of the global dynamic properties of the model in the parameter ranges where three steady states exist, reveals the existence of an attracting limit cycle surrounding the three steady states, leading to a situation of multistability, with a rich and complex dynamic structure.

Key words: Business cycle – Dynamical systems – Stability – Bifurcations

JEL Classification: C62, E32

1 Introduction

The model proposed by Kaldor (1940) is one of the earliest and simplest nonlinear models of business cycles. If compared with the modern approaches to the

business cycle (emphasizing the relevance of both the microfoundations and the explicit formal dynamic analysis), it appears very simple and rather dated. Thus this model cannot be considered a satisfying description of actual economies. Nevertheless, it continues to generate a considerable amount of economic, pedagogical and methodological interest, both from the point of view of the economist and of the applied dynamicist (see e.g. Gabisch and Lorenz, 1989).

After Kaldor (1940), the Kaldor approach to the business cycle is found in a paper by Chang and Smyth (1971), where a reformulation of the Kaldor model is offered using the language and the formalism of the theory of *dynamical systems*. In fact, Chang and Smyth proposed a representation of the mechanism described by Kaldor in the form of a *continuous time* dynamical system, expressed as a system of two nonlinear differential equations in income and capital, that shows the occurrence of periodic dynamics: the equilibrium level of income is unstable and the system fluctuates around it along a stable limit cycle (see also Grasman and Wentzel, 1994). Later, many authors reformulated the Kaldor approach to business cycle as a *discrete time* dynamical system, expressed by a system of two nonlinear difference equations (see e.g. Dana and Malgrange, 1984; Hermann, 1985; Lorenz, 1992, 1993). In this framework, more complex dynamics are evidenced, since endogenous fluctuations around the unstable equilibrium have been shown, which may be periodic, quasi periodic or even chaotic.

The idea at the basis of Kaldor (and Kaldorian) models is the following. If, at the steady state of the system, the propensity to invest is greater than the propensity to save, then the system is unstable. Such instability does not give rise to explosive dynamics, but rather causes the onset of fluctuations provided that, when the system is far from the steady state, the propensity to invest decreases until it becomes lower than the propensity to save. Kaldor argued that this happens by assuming a nonlinear sigmoid-shaped investment function. Indeed, this condition is not sufficient, because the existence of the oscillations also depends on the reaction of the firms to excess demand. So, two relevant parameters should be considered: the *speed of reaction* to the excess demand, which has a destabilizing role, and the *propensity to save*, which has a stabilizing effect.

The model we propose is expressed in the form of a discrete dynamical system, obtained by assuming that the firms' investment decisions are based on an expected "normal" value of income, which is exogenously given. Such an assumption of "exogenously given expectations" is only implicit in Kaldor (1940), and it is in perfect agreement with the Keynesian spirit of his approach.[1]

In this paper we analyze the joint dynamic effects of the two parameters mentioned above, and we show that the exogenously given equilibrium is only stable for low values of the firms' speed of reaction and sufficiently high values of the propensity to save. We also show that, if a relatively high value of the speed of adjustment is considered (but, in any case, much lower, and more realistic, than the values considered by many authors), the dynamic scenarios observed

---

[1] On the notion of " 'normal' level of activity", see Kaldor (1940), pp. 180–181.

strongly depend on the values of the propensity to save. In fact, low values of the propensity to save give rise to a situation of bi-stability, i.e. the exogenous steady state is unstable and two stable equilibria exist, each with its own basin of attraction. We show that these basins may be rather complex and intermingled. Moreover, for increasing values of the propensity to save (but, in any case, in the range of low values), global bifurcations may occur at which a stable limit cycle appears which encloses all the steady states, both the central one (unstable) and the two external ones (attracting), thus giving a situation of multi-stability. This occurs for parameter ranges that are slightly different (and we believe more realistic, being characterized by lower values of the speed of adjustment and propensity to save) with respect to the ones usually proposed in the literature on nonlinear oscillations generated by Kaldor-type models.

From the point of view of the mathematical methods, it is worth noting that the results outlined above are obtained through an analysis which is not limited to the usual study of the local stability and local bifurcations, based on the linearization of the dynamical system through the localization of the eigenvalues of the Jacobian matrix. Rather, they require a global analysis of the properties of the dynamical system, obtained through a continuous dialogue between analytic, geometric and numerical methods. This is typical of the study of the global properties of nonlinear dynamical systems of dimension greater than one, as stressed in Mira et al. (1996) and recently emphasized in Brock and Hommes (1997). In particular, the importance of homoclinic bifurcations in the global analysis of nonlinear dynamical systems, emphasized by many authors (see e.g. Guckenheimer and Holmes, 1983; Palis and Takens, 1993) has been recently stressed also in the context of dynamic economic modeling (see e.g. Gardini, 1993; Brock and Hommes, 1997; Bischi et al., 2000).

The paper is organized as follows. In Section 2, the dynamic Kaldor-like model analyzed in this paper is described, and in Section 3 the standard analysis of the steady states and their local stability properties is given, together with the analytic study of the local bifurcation curves in the space of the parameters. The main results of the paper are given in Section 4, where some global bifurcations are studied that are responsible for the creation of limit cycles and give rise to situations of coexistence of three attractors, a dynamic scenario which, up to now, has not been evidenced in the literature on dynamic Kaldor models. In Section 5, we slightly modify the dynamic equations by breaking the symmetry of the model, and we show that the global bifurcations described in Section 4 substantially persist under such structural modification. This allows us to state that the dynamic scenarios numerically observed in Section 4 are fairly robust.

2 The model

Let us consider the following discrete-time version of the Kaldor model, which closely follows Rodano (1997) (for other similar discrete-time versions see Dana and Malgrange, 1984; Hermann, 1985; Lorenz, 1992):

$$Y_{t+1} = Y_t + \alpha(I_t - S_t)$$
$$K_{t+1} = (1 - \delta)K_t + I_t \tag{1}$$

where the dynamic variables Y_t and K_t represent, respectively, the income (or output) level and the capital stock in period t. The parameter α ($\alpha > 0$) represents a *speed of adjustment*, measuring the firms' reactions to the demand excess (equivalent, in a macroeconomic environment, to the difference between investment demand (I_t) and saving (S_t)). A small value of α means a prudent reaction, which can be explained by a high degree of risk aversion or a relevant monopoly degree. Conversely, a high value of α (greater than one) means rash reactions due to a risk propensity or to competitive pressures, which can cause a coordination failure. Finally, the parameter δ ($0 < \delta < 1$) represents the *capital stock's depreciation rate*.

As usual in a Keynesian framework, savings are assumed to be proportional to the current level of income,

$$S_t = \sigma Y_t$$

where the coefficient σ, $0 < \sigma < 1$, represents the *propensity to save*. While in many versions of the Kaldor model the saving function is assumed to be non-linear, we prefer a linear specification, both for its analytical simplicity and for its sounder microfoundation. Moreover, in our case this assumption does not affect the nonlinearity of the model, which is ensured by the nonlinearity of the investment function, given below.

As usual, the investment demand is assumed to be an increasing and sigmoid-shaped function of income. Without loss of generality, in the following we shall consider the form proposed in Rodano (1997)

$$I_t = \sigma\mu + \gamma \left(\frac{\sigma\mu}{\delta} - K_t\right) + \arctan(Y_t - \mu) \tag{2}$$

where $\sigma\mu/\delta$ is the "normal" level of capital stock. In equation (2), two short run investment components are considered: the first one is proportional to the difference between normal capital stock and current stock, according to a coefficient γ ($\gamma > 0$), usually explained by the presence of adjustment costs; the second one is an increasing, but not linear, function of the difference between current income and its "normal" level. This "normal" level of income, again in the logic of Keynesian setups, is exogenously assumed in firm expectations. We indicate this normal level of income with the parameter μ ($\mu > 0$). Therefore, since the expected income $Y_t^e = \mu$, $\sigma\mu$ represents the normal level of savings.[2] This second component of the short run investment function is a convenient specification of the sigmoid-shaped relationship between investment and income proposed by Kaldor. We note that this analytic specification does not compromise the generality of the results.

By substituting the expressions of I_t and S_t into the dynamic model (1), we get that the time evolution of income and capital is determined by the iteration of a two-dimensional nonlinear map $T : (Y_t, K_t) \rightarrow (Y_{t+1}, K_{t+1})$ given by:

---

[2] In other words, firms know the propensity to save, σ, and thus the *normal* (or expected) level of savings, but not the *actual* level.

$$T : \begin{cases} Y' = Y + \alpha \left[\sigma\mu + \gamma \left(\frac{\sigma\mu}{\delta} - K \right) + \arctan(Y - \mu) - \sigma Y \right] & \text{(a)} \\ K' = (1 - \delta)K + \sigma\mu + \gamma \left(\frac{\sigma\mu}{\delta} - K \right) + \arctan(Y - \mu) & \text{(b)} \end{cases} \quad (3)$$

where the symbol $'$ denotes the unit time advancement operator.

In the following, we study the qualitative dynamical properties of the map (3), and try to explore and to explain the different kinds of transient and long-run behavior that characterize the model for economically meaningful parameter constellations. In addition to the usual local stability analysis, based on the linear approximation of the map at the steady states, we analyze some global dynamical properties and stress the role of some global bifurcations that explain the occurrence of new dynamic scenarios.

3 Fixed points and local stability analysis

The equilibrium points (or steady states) of the model (1) are the fixed points of the map T, solutions of the algebraic system:

$$\begin{cases} \sigma\mu + \gamma \left(\frac{\sigma\mu}{\delta} - K \right) + \arctan(Y - \mu) - \sigma Y = 0 \\ \sigma\mu + \gamma \left(\frac{\sigma\mu}{\delta} - K \right) + \arctan(Y - \mu) - \delta K = 0 \end{cases},$$

obtained by setting $Y' = Y$ and $K' = K$ in (3). This system can be rewritten as:

$$\begin{cases} K = \frac{\sigma}{\delta} Y \\ \sigma \left(1 + \frac{\gamma}{\delta} \right) (Y - \mu) = \arctan(Y - \mu) \end{cases}. \quad (4)$$

The first equation says that the fixed points belong to the line $K = \frac{\sigma}{\delta} Y$, and from the second equation we have that the equilibrium values of Y can be obtained as intersections between the line of equation $z = \sigma \left(1 + \frac{\gamma}{\delta} \right) (Y - \mu)$ and the sigmoid-shaped graph of the function $z = \arctan(Y - \mu)$. Such intersections may be one or three according to the value of the aggregate parameter $\sigma \left(1 + \gamma/\delta \right)$: if $\sigma \left(1 + \gamma/\delta \right) \geq 1$, then the exogenously given equilibrium $P = (\mu, \mu\frac{\sigma}{\delta})$ is the unique steady state, whereas in the complementary case $\sigma \left(1 + \gamma/\delta \right) < 1$, two further steady states exist, say R and Q, located in symmetric positions with respect to the point P, given by $R = (Y_R, \frac{\sigma}{\delta} Y_R)$ and $Q = (Y_Q, \frac{\sigma}{\delta} Y_Q)$, with $Y_Q = 2\mu - Y_R$, $Y_R < \mu$ being the smallest real solution of the second equation in (4), which can be computed by any numerical method for finding the real roots of an equation. It is trivial to realize that the steady states are independent of the adjustment parameter α.

It is worth noting that the steady state P can be interpreted as a full equilibrium because the agents expectations about the normal levels of income and capital are realized, whereas the other equilibrium points, Q and R, must be interpreted as temporary equilibria because, given expectations, investment and saving are equal, but the expectations are not realized.

Let us now consider the local stability of the fixed point $P = (\mu, \mu\frac{\sigma}{\delta})$. As usual, the analysis of the local stability of a fixed point is obtained through the localization, in the complex plane, of the eigenvalues of the Jacobian matrix evaluated at the fixed point, and their dependence on the parameters of the model. In the following, we consider the parameters δ and γ as fixed, and we study the stability regions, and the local bifurcation curves, in the space of the parameters α, σ, with $\alpha > 0$ and $0 < \sigma < 1$. In order to simplify the mathematical treatment, we assume that the parameter γ belongs to the range $0 < \gamma < 2 - \delta$, a condition satisfied in economically feasible situations, being usually $\gamma < 1$. The results of the standard analysis of the eigenvalues, given in the appendix A.1, together with the above arguments concerning the existence of the fixed points of the map T, allow us to state the following proposition (see also Fig. 1).

Proposition 1

(i) If $\sigma \geq \sigma_p$, with

$$\sigma_p = \frac{\delta}{\delta + \gamma} \tag{5}$$

then the point $P = (\mu, \mu\frac{\sigma}{\delta})$ is the unique fixed point of the map T, and if $\sigma < \sigma_p$ then two further fixed points exist, symmetric with respect to the point P.

(ii) If $\gamma < 2 - \delta$, the point P is locally asymptotically stable if the parameters α and σ belong to the region ABCD of the plane (α, σ), with vertices $A = \left(0, \frac{\delta}{(\delta + \gamma)}\right)$, $B = (0, 1)$, $C = \left(\frac{\delta + \gamma}{\gamma}, 1\right)$, $D = \left(\frac{(\delta + \gamma)^2}{\gamma}, \frac{\delta}{\delta + \gamma}\right)$, where the sides AD and CD belong to the line $\sigma = \sigma_p$ and the hyperbola of equation[3]

$$\sigma = \sigma_{hP}(\alpha) = \frac{1 - \delta}{1 - \delta - \gamma} - \frac{\gamma + \delta}{\alpha(1 - \delta - \gamma)} \tag{6}$$

respectively.

(iii) If the point (α, σ) exits the stability region ABCD by crossing the side AD, then a supercritical pitchfork bifurcation occurs at which the fixed point P becomes a saddle point and two stable nodes are created near it; if the point (α, σ) exits the stability region ABCD by crossing the side CD, then a Hopf bifurcation occurs at which the fixed point P is transformed from a stable focus to an unstable focus[4].

This proposition, concerning the usual local analysis, i.e. based on the linear approximation of dynamical system near a steady state, seems to imply that for values of the parameters below the line $\sigma = \sigma_p$, where three equilibria exist,

---

[3] Figure 1 describes the case $\gamma + \delta < 1$. In the case $\gamma + \delta > 1$ the abscissa of the vertex C is lower than the abscissa of D and the branch of hyperbola through C and D is negatively sloped (but the concavity of the Hopf curve does not change). In the particular case $\gamma + \delta = 1$, the side CD belongs to the vertical line $\alpha = 1/\gamma$.

[4] Numerical simulations with parameter values (α, σ) taken just after the crossing of the Hopf curve CD show the existence of an attracting closed invariant curve around the unstable focus (on which the dynamics may be periodic or quasi-periodic), thus revealing the *supercritical* nature of the Hopf bifurcation. See also Appendix A1.
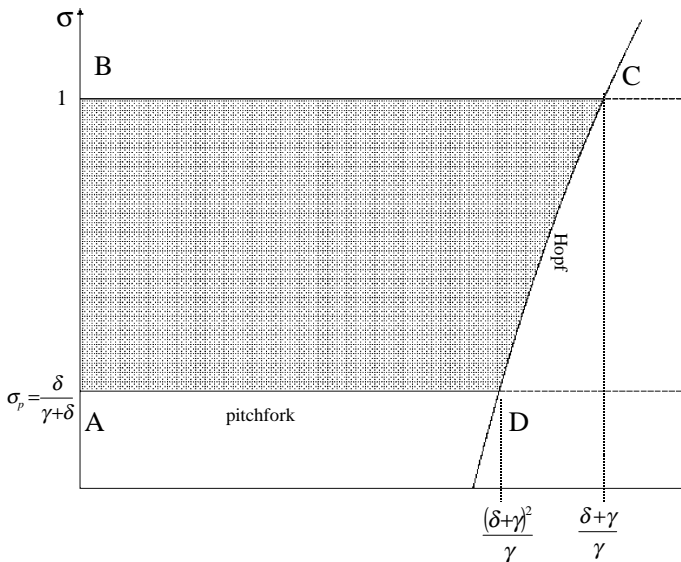
Fig. 1. The shaded region *ABCD* represents, according to Proposition 1, the domain of stability of the steady state *P* in the plane of the parameters α and σ. This figure is obtained with $\delta + \gamma < 1$, namely $\delta = 0.2$ and $\gamma = 0.6$. In the case $\delta + \gamma > 1$ the abscissa of the vertex *C* is less that the abscissa of the vertex *D*, hence the branch of hyperbola through *C* and *D* is negatively sloped

situations of bi-stability (without oscillations) are obtained. By contrast, self-sustained oscillatory behaviors seem to appear only for sufficiently high values of the propensity to save, i.e. above the line $\sigma = \sigma_p$, and for increasing values of the adjustment parameter α, i.e. when the curve *CD* of Figure 1 is crossed. Indeed, in the rich literature on dynamical systems that represent Kaldor-like business cycle models, this is the stream followed by many authors: both in discrete time and in continuous time, stable oscillations along limit cycles, generated via Hopf bifurcations, are considered for sufficiently high values of α and σ. However, small values of the propensity to save, σ, are more realistic, and hence it makes sense to wonder if oscillatory dynamics can be obtained in the region of the parameter space where three equilibria exist. This is the reason why, in the next section, we focus our attention on the region of the parameter space in which three equilibria exist, and we consider some global dynamic properties, and global bifurcations, by extending our analysis far from the local bifurcation curves. The method used to perform this analysis will require an interplay among analytic, geometric and numerical techniques, a "modus operandi" that is typical for the study of the global dynamic properties of nonlinear dynamical systems of dimension greater than one, as stressed in Mira et al. (1996), Abraham et al. (1997), and Brock and Hommes (1997).

4 Global dynamics with three coexisting equilibria

In this section, we explore the global dynamic behaviors of the model when the values of the parameters are out of the region of stability of the exogenously given equilibrium P, and in the set of parameters such that the three equilibria R, P, and Q exist. We stress that our numerical explorations will be limited to the following ranges for the parameters, which we claim to be rather realistic from the point of view of their economic meaning: $0 < \alpha \le 6$; $0.1 \le \delta \le 0.2$; $0.5 \le \gamma \le 0.9$; $0.1 \le \sigma \le 0.4$. The equilibrium level μ is an exogenous constant, and we have assumed $\mu = 10$ in all our numerical simulations.

In the following, without loss of generality, we consider fixed values of the parameters δ and γ, given by $\delta = 0.2$ and $\gamma = 0.6$, and we note some local and global bifurcations observed through numerical explorations by following particular bifurcation-routes in the parameter plane (α, σ). With these values of the parameters δ and γ we have $\sigma_p = 0.25$, $\frac{(\delta+\gamma)^2}{\gamma} = 1.0\overline{6}$, $\frac{\delta+\gamma}{\gamma} = 1.\overline{3}$. Since $\delta + \gamma < 1$, we refer to the situation shown in Figure 1, where $\frac{(\delta+\gamma)^2}{\gamma} < \frac{\delta+\gamma}{\gamma}$. Of course, similar results can be applied to the case $\delta + \gamma > 1$, just reversing the above inequality.
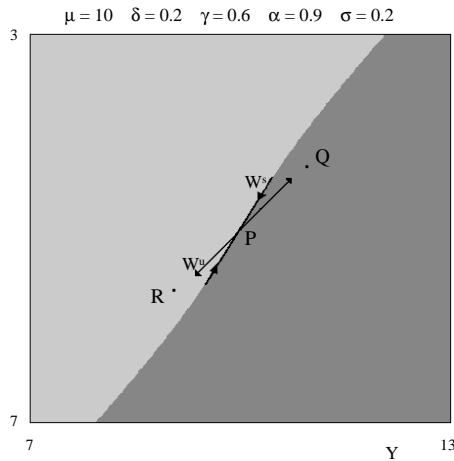
$\mu = 10 \quad \delta = 0.2 \quad \gamma = 0.6 \quad \alpha = 0.9 \quad \sigma = 0.2$

Fig. 2. For $\mu = 10$, $\delta = 0.2$, $\gamma = 0.6$, $\alpha = 0.9$ and $\sigma = 0.2 < \sigma_p$ three fixed points exist: P is a saddle point, R and Q are stable nodes. The two different colors represent the basins of attraction $\mathcal{B}(R)$ and $\mathcal{B}(Q)$ of the stable steady states R and Q, respectively. The boundary that separates the two basins is the stable set of the saddle point P

We first consider a value of the adjustment coefficient α taken in the range $0 < \alpha < (\delta+\gamma)^2/\gamma$, for example $\alpha = 0.9$. According to Proposition 1, the point P is stable for $\sigma_p < \sigma < 1$, and for $\sigma < \sigma_p$, just after the supercritical pitchfork bifurcation, we have a situation of bi-stability: two fixed points R and Q exist and are stable (stable nodes), and the fixed point P is a saddle point. The stable set of P, $W^s(P)$, acts as a basin boundary, i.e. it separates the basins of attraction of R and Q, say $\mathcal{B}(R)$ and $\mathcal{B}(Q)$ respectively. This can be clearly seen in Figure 2,

μ = 10   δ = 0.2   γ = 0.6   α = 1.2   σ = 0.2378
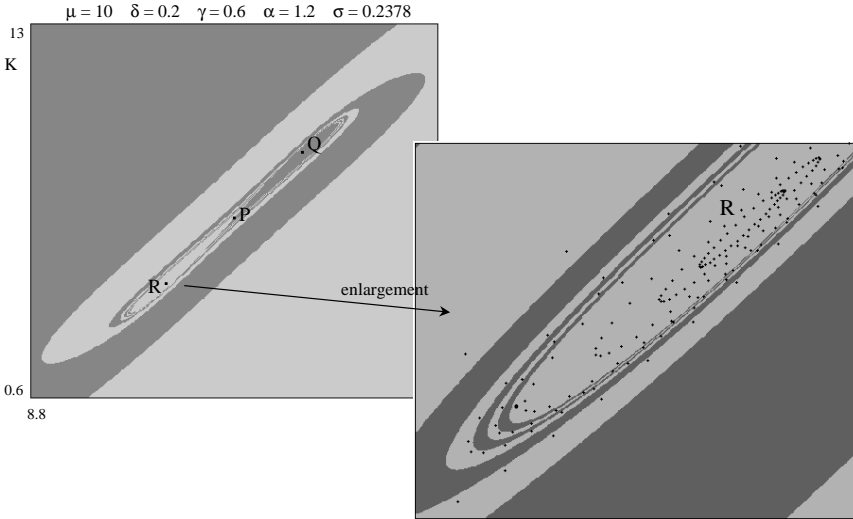
Fig. 3. For $\alpha = 1.2$ and $\sigma = 0.2378$, the fixed point P is a saddle point and R and Q are stable foci. The stable set of the saddle P, which separates the basins $\mathscr{B}(R)$ and $\mathscr{B}(Q)$, is now more involved with respect to the situation shown in Figure 2. The meaning of the colors is the same as in Figure 2. The enlargement shows how a trajectory can reach the fixed point R without crossing the basin boundary with Q

where the light grey region represents the basin $\mathscr{B}(R)$, i.e. the set of points that generate trajectories converging to R, and the dark grey region represents the basin $\mathscr{B}(Q)$, i.e. the set of points that generate trajectories converging to Q. In Figure 2 also the portions of the stable and unstable sets issuing from the saddle P are represented, denoted by W^s and W^u, respectively. It is important to stress that the points R and Q represent temporary equilibria, where expectations are not realized; however, in our model we assume that the level of expectations is exogenously given, so the model cannot say how such expectations change when they are wrong.

Now we consider a higher fixed value of α, such that $(\delta + \gamma)^2/\gamma < \alpha < (\delta + \gamma)/\gamma$, for example $\alpha = 1.2$. In this case P is locally stable for $\sigma > \sigma_{hP}$, where $\sigma_{hP} = 0.\overline{6} > \sigma_p$ according to (6). As stressed above, we are mainly interested in the range $0 < \sigma < \sigma_p$, where the unstable equilibrium P coexists with the other two equilibria R and Q. Indeed, as σ varies in this range, some interesting bifurcations occur, which are associated with the existence of the two other fixed points, R and Q. These bifurcations can be observed and described by following, for example, the bifurcation path obtained by increasing the parameter σ along the line $\alpha = 1.2$.

Also in this case, for low values of σ, P is a saddle point, the other two equilibria R and Q are locally stable (stable nodes) and their basins are qualitatively similar to those shown in Figure 2. As σ is increased, the two fixed points R and Q are transformed from stable nodes into stable foci (i.e. the eigenvalues of their Jacobian matrix become complex conjugate, see Appendix **A1**) and the stable
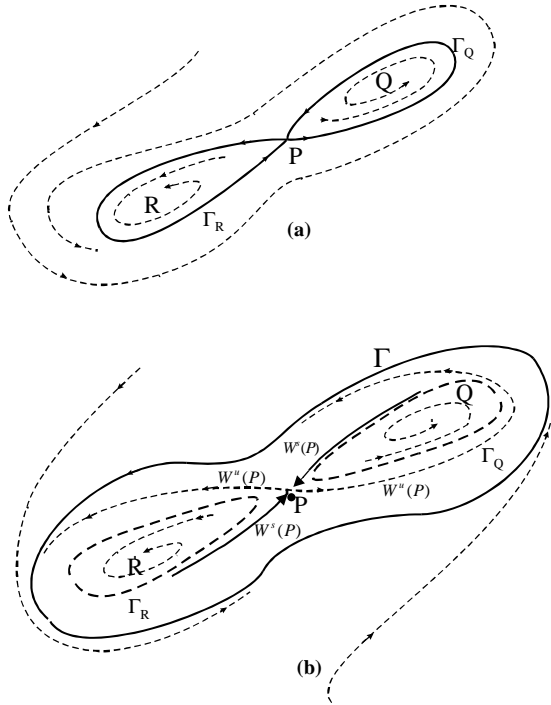
Fig. 4. a At the global bifurcation value $\sigma = \sigma_g$, a homoclinic connection is created by the stable and unstable sets of the saddle fixed point P. The trajectories starting outside of the eight-shaped curve Γ tend to Γ, while those starting inside converge to R or Q. **b** Just after the bifurcation three closed invariant curves exist. Two of them, Γ_R and Γ_Q, are repelling (the thicker dashed curves) and bound the basins of the stable equilibria R and Q, respectively. The larger closed invariant curve, represented by a thick and continuous line, is attracting. $W^s(P)$ and $W^u(P)$ denote the stable and unstable manifolds of the saddle P, respectively

set $W^s(P)$, as well as the unstable set $W^u(P)$, become more involved, because they wing around the fixed points R and Q. Consequently, the basin boundaries appear to be more complicated, as shown in Figure 3, obtained for $\alpha = 1.2$ and $\sigma = 0.2378$. This situation of bi-stability is characterized by a greater uncertainty about the long-run behavior of a trajectory starting from a given initial condition. In fact, a slight perturbation of an initial condition, taken in the region around P, may cause a crossing of the basin boundary, and consequently it may have the effect of causing the convergence to a different equilibrium.

The geometric shape of the stable and unstable sets $W^s(P)$ and $W^u(P)$ suggests that a global bifurcation is going to occur. In fact, as σ is slightly increased with respect to the value used in fig. 3, a global bifurcation occurs at $\sigma = \sigma_g \simeq 0.23799$, which gives rise to two homoclinic orbits of P, as qualitatively shown in Figure 4a. This is a typical homoclinic bifurcation (see e.g. Abraham et al., 1992, Palis and Takens, 1993): the stable and unstable sets join, thus giving rise to a pair of closed invariant curves through P, denoted as Γ_R and Γ_Q in Figure 4a. At the homoclinic bifurcation, the closed curve $\Gamma = \Gamma_R \cup \Gamma_Q$

is an attracting set from outside, and repelling from the inside: the area bounded by Γ_R is the basin of attraction of the stable focus R, while the area bounded by Γ_Q is the basin of attraction of Q. As σ is slightly increased above σ_g, we have three closed invariant curves (see Fig. 4b): Γ_R and Γ_Q, which are two closed *repelling* invariant curves surrounding R and Q respectively, bounding the basins of attraction $\mathscr{B}(R)$ and $\mathscr{B}(Q)$, and Γ, which is a larger *attracting* limit cycle that surrounds the three fixed points.

The dynamic scenario observed just after the homoclinic bifurcation is shown in Figure 5a, where the basins of the three coexisting attractors R, Q, and Γ are represented by different colors: $\mathscr{B}(R)$ and $\mathscr{B}(Q)$ are light and dark grey, respectively, as in the previous pictures, while $\mathscr{B}(\Gamma)$ is white. In Figure 5b three typical trajectories, starting from initial conditions taken in the three different basins, are represented versus time: starting from an initial condition in $\mathscr{B}(R)$ or $\mathscr{B}(Q)$ the long-run evolution of the system is characterized by damped oscillations converging to the respective steady states, whereas starting from an initial condition in $\mathscr{B}(\Gamma)$, quasi-periodic self-sustained oscillations are seen in the long run.

It is worth noting the remarkable change which occurs in the dynamics of T as σ crosses this bifurcation value σ_g: for $\sigma < \sigma_g$ any point of the phase plane generates a trajectory converging to either one of the equilibria Q or R[5], and we have wide basins of the two coexisting stable equilibria (see the situation shown in Fig. 3), whereas for $\sigma > \sigma_g$ the majority of the trajectories are converging to an oscillating behavior, and the basins of Q and R reduce to small regions enclosed by the limit cycle Γ (Fig. 5a).
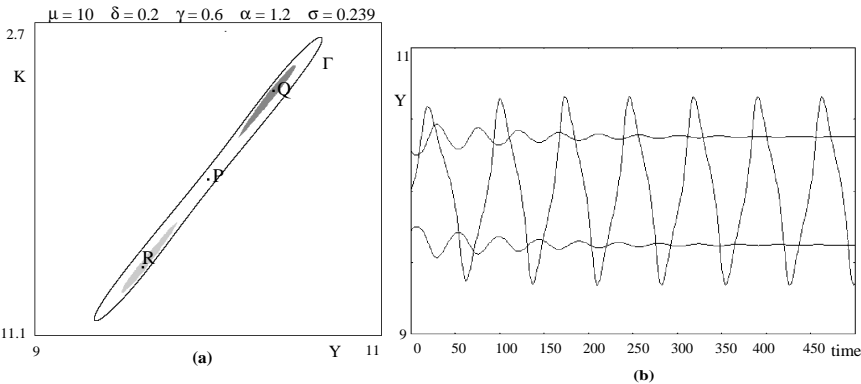
Fig. 5. a For $\alpha = 1.2$ and $\sigma = 0.239$, i.e. $\sigma_g < \sigma < \sigma_{hQR}$, the fixed point P is a saddle point and R and Q are stable foci. The basins $\mathscr{B}(R)$ and $\mathscr{B}(Q)$, represented by light grey and dark grey regions respectively, are bounded by two repelling closed invariant curves. All the points in the white region generate trajectories converging to a limit cycle Γ. **b** Three sequences Y_t, obtained by the iteration of the map (3), starting from initial conditions belonging to the basins $\mathscr{B}(\Gamma)$, $\mathscr{B}(R)$ and $\mathscr{B}(Q)$, are plotted versus time for $0 \leq t \leq 500$

---

[5] Apart from the points belonging to the stable set of the saddle P.

As σ increases, we know that the two fixed points R and Q shall merge with P (and disappear) at $\sigma = \sigma_p$. At σ_p these two fixed points must have real eigenvalues $z_1 = 1$ and $z_2 > 1$, since they merge with the unstable fixed point P. This implies that some other bifurcation must occur between σ_g and σ_p, at which the equilibria R and Q lose their stability. In fact, as $\sigma > \sigma_g$ increases, we observe that the two closed repelling invariant curves Γ_R and Γ_Q become smaller and smaller, and consequently also the basins $\mathcal{B}(R)$ and $\mathcal{B}(Q)$ decrease in size, until σ reaches a bifurcation value $\sigma_{hRQ} \simeq 0.2407$ at which a subcritical Hopf bifurcation of R and Q occurs, i.e. at $\sigma = \sigma_{hRQ}$ the two closed repelling curves merge with the fixed points, and for $\sigma > \sigma_{hRQ}$ the fixed points R and Q become unstable (repelling foci). The only surviving attractor is now the closed invariant curve Γ. In this situation, the system converges to the limit cycle Γ that surrounds the three unstable equilibria. Such an attractor (see Fig. 6) can be considered a full equilibrium of the system because the expectations are realized *on average*, and so the agents have no reason to change them.
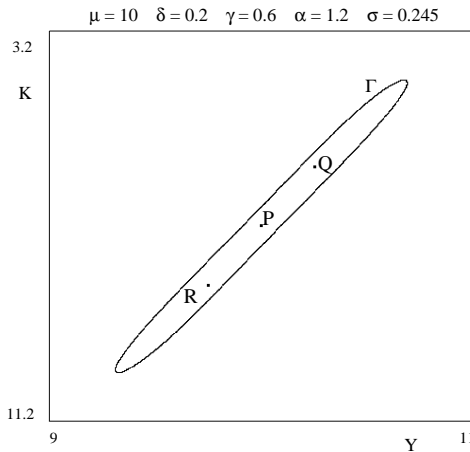
Fig. 6. For $\alpha = 1.2$ and $\sigma = 0.245$, i.e. $\sigma_{hQR} < \sigma < \sigma_p$, all the three fixed points are unstable, and the only attractor is the limit cycle Γ that surrounds them

As σ is further increased, the repelling foci R and Q become repelling nodes, merge with the fixed point P at $\sigma = \sigma_p$, and then disappear, leaving the only fixed point P, repelling node, surrounded by a closed attracting curve Γ. Then, if we further increase σ, the limit cycle Γ becomes smaller and smaller, and shrinks into P when the stability region in the parameter space is reached, say at $\sigma = \sigma_{hP}$, where a supercritical Hopf bifurcation of P occurs[6], according to Proposition 1 (see also Fig. 1). Then P remains the only attractor for higher values of σ.

---

[6] In the prototype textbook examples of *supercritical* Hopf bifurcations, a stable limit cycle bifurcates from a fixed point when a parameter is increased. Here this bifurcation is described following the opposite path, with the disappearance of the cycle for an increased value of σ: in this case the term *inverse supercritical* is occasionally used in the literature.
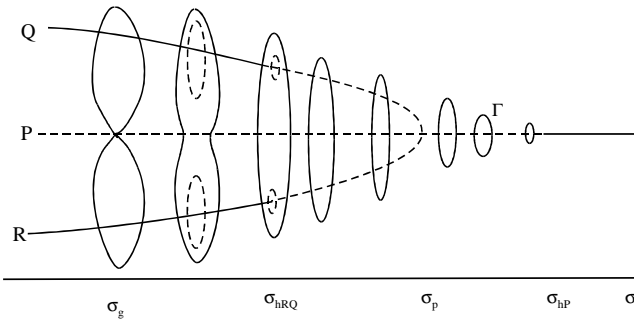
Fig. 7. Bifurcation diagram that qualitatively represents the dynamic scenarios and the bifurcations that are met along the path with fixed $\alpha = 1.2$ and σ varying in the range $(0, 1)$. The parameter σ varies along the horizontal axis. The solid lines represent attracting sets, the dashed lines repelling sets

This sequence of numerically observed bifurcations can be summarized by a bifurcation diagram, as in Figure 7, where the parameter σ varies along the horizontal axis. In this figure the solid lines represent attracting sets, the broken lines repelling sets. Clearly, we can describe the bifurcation diagram of Figure 7 as σ decreases from 1 to 0 as well. At first, for $\sigma > \sigma_{hP}$, the only attractor is the stable fixed point P, which becomes unstable at σ_{hP} via a supercritical Hopf bifurcation. As is well known, the results of the Hopf theorem are only local (i.e. they hold for parameters' values close to the Hopf bifurcation curve) so the existence of Γ is proved only for a small neighborhood of σ, and in general nothing can be said about the fate of the attracting curve Γ as the parameters move far from the bifurcation value. However, our numerical explorations show that the invariant curve Γ survives for decreasing σ, even after the fixed points R and Q are created at $\sigma = \sigma_p$, and even after their subcritical Hopf bifurcation occurs, which transforms them into stable fixed points and gives rise to the repelling closed invariant curves Γ_R and Γ_Q that constitute the boundaries of their basins of attraction. However, as Γ_R and Γ_Q increase in size, they ultimately merge with Γ, causing their disappearance and that of Γ as well, leaving the attracting fixed points R and Q. After this, a situation of bi-stability, without persistent self-sustained oscillations, characterizes the dynamics of the model.

A similar behavior can be observed for $\alpha > (\delta + \gamma)/\gamma$ as well, because the attracting closed invariant curve created at the supercritical Hopf bifurcation still exists for $\sigma < 1$ even if such bifurcation occurs at $\sigma = \sigma_{hP} > 1$, i.e. outside the economically meaningful range of σ. The only difference is that for $\alpha > \frac{\delta + \gamma}{\gamma}$ the fixed point P is unstable for any value of σ, $0 < \sigma < 1$.

We also remark that a global bifurcation, similar to the one described above, also occurs if we fix σ at a value $\bar{\sigma} < \sigma_p$ and we increase the value of the adjustment parameter α. At low values of α, the dynamics are those associated with two attracting fixed points the basins of attraction of which are separated by the stable set $W^s(P)$ of the saddle point P. Then a homoclinic bifurcation deeply
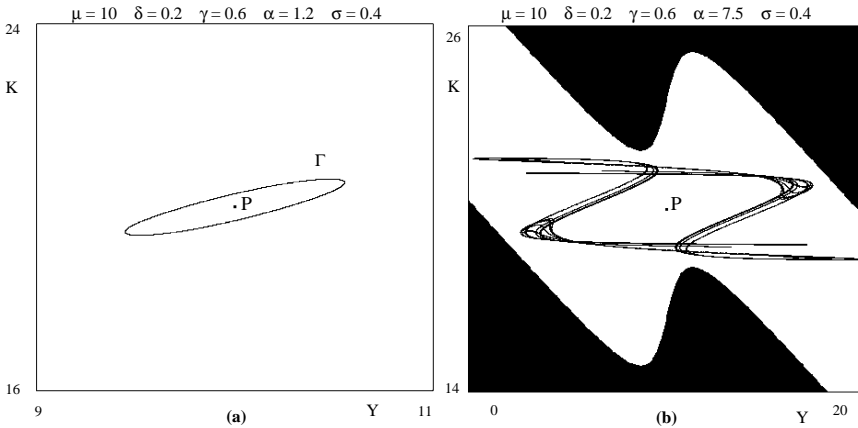
Fig. 8. a For $\alpha = 1.2$ and $\sigma = 0.4$, i.e. $\sigma_p < \sigma < 1$, P is the unique steady state, an unstable focus, and the unique attractor is the limit cycle Γ. **b** For the same value of σ as in **a** and a much greater value of α, $\alpha = 7.5$, a chaotic attractor exists around the unstable equilibrium P. The black region represents the basin of infinity, i.e. the set of points which generate divergent trajectories

modifies the two basins when α is increased. Also in this case, the homoclinic bifurcation has a striking effect on the dynamics of the model: most of the trajectories that were previously converging to a fixed point, move on self-sustained oscillations soon after the bifurcation.

As a final remark, we stress that in the several studies of the dynamical systems which have been proposed in the literature to represent the Kaldor business cycle model, both in continuous and discrete time, self-sustained oscillations are observed for increasing values of the reaction parameter α, when only one steady state exists. Indeed, especially with discrete time dynamic models, when increasing values of α are considered, more and more complex attractors (often characterized by chaotic dynamics) appear around the unstable fixed point P. Of course, similar situations are obtained with our model as well, as shown in Figure 8.

The two situations shown in Figures 8a and 8b are obtained with the same value of σ, $\sigma = 0.4 > \sigma_p$, so that only the equilibrium P exists, and two different values of the reaction parameter, namely $\alpha = 1.2$ in Figure 8a and $\alpha = 7.5$ in Figure 8b. In Figure 8b, which is typical in the literature on discrete-time Kaldor models, the initial conditions taken in the white region generate trajectories that exhibit chaotic oscillations around P in the long-run, whereas the black region represents the set of points that generate diverging trajectories, i.e. the basin of infinity. We observe that in the situations obtained with small values of the speed of adjustment α, as in Figures 6 and 8a, the wide limit cycle appears to be a global attractor, i.e. all the numerically generated trajectories starting out of it are seen to converge to it. Instead, as often observed in the literature (see e.g. Lorenz, 1992), diverging trajectories can be obtained when higher values of the adaptive parameter α are used. This is the case shown in Figure 8b. Of course, such trajectories cannot represent economically feasible evolutions of the system,

and their presence indicates that the model is less reliable for high values of α. As expected, if α is further increased, the basin of infinity enlarges until it covers almost the whole phase plane, i.e. any bounded attractor disappears.

5 Breaking the symmetry

It is interesting to investigate whether the creation (through the global homoclinic bifurcation) and the permanence of the limit cycle Γ around the three steady states is related to the symmetry property of T (see Appendix B). Indeed, from the particular geometric shape of the stable and unstable sets of the saddle fixed point P, which lead to the formation of the homoclinic orbit shown in Figure 4a, it seems that the symmetry of the map may play some important role. In order to show the robustness of the dynamic phenomena analyzed in Section 4, we introduce a structural change in the model that breaks its symmetry. To this end, without changing the basic assumptions of the model, we slightly modify the S-shaped investment function in such a way that the resulting map is no longer symmetric, by defining:

$$\widetilde{I}(Y,K) = \sigma\mu + \gamma \left(\frac{\sigma\mu}{\delta} - K \right) + a(Y) , \tag{7}$$

where:

$$a(Y) = \begin{cases} \arctan(Y - \mu) & \text{if } Y \geq \mu \\ \theta \arctan(Y - \mu) & \text{if } Y < \mu \end{cases} . \tag{8}$$

It is plain that for $\theta = 1$ we have $\widetilde{I}(Y,K) = I(Y,K)$, i.e. we get the function (2) symmetric with respect to $Y = \mu$, whereas $\theta \neq 1$ introduces a "symmetry breaking" which also breaks the symmetry of the map [7]. In fact, replacing $I(Y,K)$ with $\widetilde{I}(Y,K)$ we obtain a new map, say $\widetilde{T} : (Y,K) \to (Y',K')$, defined as

$$(Y',K') = \widetilde{T}(Y,K) = \begin{cases} T(Y,K) & \text{if } Y \geq \mu \\ T_\theta(Y,K) & \text{if } Y < \mu \end{cases} , \tag{9}$$

where T is the map already defined in (3) and

$$T_\theta : \begin{cases} Y' = Y + \alpha \left[\sigma\mu + \gamma \left(\frac{\sigma\mu}{\delta} - K \right) + \theta \arctan(Y - \mu) - \sigma Y \right] & \text{(a)} \\ K' = (1 - \delta)K + \sigma\mu + \gamma \left(\frac{\sigma\mu}{\delta} - K \right) + \theta \arctan(Y - \mu) & \text{(b)} \end{cases} . \tag{10}$$

The map $\widetilde{T}$ is continuous in the whole plane but not differentiable on the line of equation $Y = \mu$. This raises some questions about the dynamic behavior, in particular related to the fact that the exogenously given fixed equilibrium $P = \left(\mu, \frac{\sigma}{\delta}\mu \right)$ belongs to the line of non-differentiability..

---

[7] This asymmetry can be justified on economic grounds as follows. The upper asymptote represents the ceiling for positive investment, whereas the lower one represents the floor for net disinvestment. They can be different since the former depends on the full employment productive capacity, while the latter is limited by the fact that gross investment cannot be negative.

Following the same method of analysis as in the symmetric case, we first consider the problems of existence and stability of the fixed points of the map $\widetilde{T}$ and then describe the global dynamics obtained by iterating the map $\widetilde{T}$, especially in the ranges of parameters such that several equilibria coexist. We shall see, in particular, that the local and global bifurcations that lead to the creation and permanence of a large amplitude limit cycle surrounding the coexisting equilibria still occur.

5.1 Fixed points of $\widetilde{T}$ and their local stability

The fixed points of $\widetilde{T}$ are obtained as solutions of $\widetilde{T}(Y, K) = (Y, K)$, equivalent to the equations $(Y, K) = T(Y, K)$ with $Y \geq \mu$ and $(Y, K) = T_\theta(Y, K)$ with $Y < \mu$, which, after simple algebraic computations, are reduced to the following system:

$$\begin{cases} K = \frac{\sigma}{\delta} Y \\ \sigma \left(1 + \frac{\gamma}{\delta}\right)(Y - \mu) = a(Y) \end{cases} , \tag{11}$$

where $a(Y)$ is the function defined in (8). Differently from the case analyzed in Section 3, now the intersections of the line $z = \sigma \left(1 + \frac{\gamma}{\delta}\right)(Y - \mu)$ with the S-shaped function $z = a(Y)$, which give the Y-coordinates of the fixed points of $\widetilde{T}$, may be one or two or three, as can be seen from a simple graphical analysis. For example, in the case $\theta > 1$, if $\sigma \left(1 + \frac{\gamma}{\delta}\right) \geq \theta$ then we have the unique fixed point, say $P = \left(\mu, \frac{\sigma}{\delta}\mu\right)$; if $1 \leq \sigma \left(1 + \frac{\gamma}{\delta}\right) < \theta$ we have one further fixed point, say $R = (Y_R, \frac{\sigma}{\delta}Y_R)$, with $Y_R < \mu$; and for $0 < \sigma \left(1 + \frac{\gamma}{\delta}\right) < 1$ we have three fixed points: P, R and $Q = (Y_Q, \frac{\sigma}{\delta}Y_Q)$ with $Y_Q > \mu$. Similar considerations can be made for the case $\theta < 1$.

It can be observed that, in our modified model, the number of fixed points of the map changes by one at each bifurcation value $\sigma = \sigma_p$ and $\sigma = \theta\sigma_p$, where σ_p is given in (5). This does not generally occur for continuously differentiable maps: for instance, in the standard pitchfork bifurcation, the number of fixed points changes from one to three. Moreover, in this case the fixed point P belongs to the line $Y = \mu$, where the map is $\widetilde{T}$ is not differentiable, and this implies that the local stability analysis of the fixed point P is not typical because we have two different Jacobian matrices of $\widetilde{T}$ in any neighborhood of P, according to $Y > \mu$ or $Y < \mu$. In other words, the local dynamics around P depend on both the Jacobians DT and DT_θ, defined in eq. (12) and (19) of the Appendix A, governing the local dynamics on the right and on the left of P, respectively.

On the contrary, when the fixed points R or Q exist, their local stability analysis is the usual one because R always belongs to the half-plane $Y < \mu$, so that we only have to consider the eigenvalues of the Jacobian matrix $DT_\theta(R)$. Q always belongs to the half-plane $Y > \mu$, so we only have to consider the eigenvalues of the Jacobian matrix $DT(Q)$.

The arguments given above about the existence of fixed points, and the study of the eigenvalues of the Jacobian matrices of $\widetilde{T}$ given in the Appendix A, allow us to state the following

Proposition 2. *The map $\widetilde{T}$ has always the fixed point $P = (\mu, \frac{\sigma}{\delta}\mu)$. One or two more fixed points, $R = (Y_R, \frac{\sigma}{\delta}Y_R)$, with $Y_R < \mu$ and $Q = (Y_Q, \frac{\sigma}{\delta}Y_Q)$ with $Y_Q > \mu$, may exist depending upon the parameter values. Let $\sigma_p = \frac{\delta}{\delta+\gamma}$. If $\theta > 1$ then*

- *for $\sigma > \theta\sigma_p$, $\widetilde{T}$ has the unique fixed point P;*
- *for $\sigma_p < \sigma < \theta\sigma_p$, $\widetilde{T}$ has the two fixed points: R and P;*
- *for $0 < \sigma < \sigma_p$, $\widetilde{T}$ has the three fixed points R, P and Q.*

  If $\theta < 1$ then

- *for $\sigma > \sigma_p$, $\widetilde{T}$ has the unique fixed point: P;*
- *for $\theta\sigma_p < \sigma < \sigma_p$, $\widetilde{T}$ has the two fixed points P and Q;*
- *for $0 < \sigma < \theta\sigma_p$, $\widetilde{T}$ has three fixed points: R, P and Q.*

If $\theta > 1$ (resp. $\theta < 1$) the stability region of the fixed point P under the map $\widetilde{T}$ is decreased (resp. increased) with respect to the stability region of P under the map T.

The statement on the stability region of P immediately follows from the comparison of the bifurcation curves defined in the Appendix A.2 with those defined in A.1. If both the eigenvalues of $DT(P)$ and $DT_\theta(P)$ have modulus less than 1, then P is locally asymptotically stable according to the classical (or topological) Lyapunov definition, i.e. a neighborhood of P exists the points of which generate trajectories that converge to P, whereas when at least one eigenvalue, both of $DT(P)$ or $DT_\theta(P)$, is in modulus greater than 1, then P is unstable.
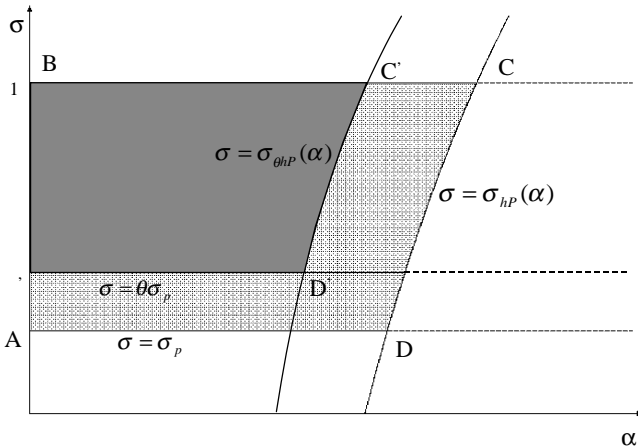
Fig. 9. Non-symmetric model. The dark grey region $A'BC'D'$ represents the domain of stability of the steady state P in the plane of the parameters α and σ. This figure is obtained with $\theta > 1$, namely $\theta = 1.2$, and $\delta + \gamma < 1$, namely $\delta = 0.2$ and $\gamma = 0.6$. In the light grey region both the eigenvalues of $DT(P)$ are in modulus less than one, but $DT_\theta(P)$ has at least one eigenvalue greater than one in modulus: in this region the steady state P is not locally asymptotically stable in the classical Lyapunov sense

However, we notice that, for the map $\widetilde{T}$, there are regions in the parameter space for which both the eigenvalues of one Jacobian matrix are less than one in modulus, while for the other matrix at least one eigenvalue z is such that $|z| > 1$. This occurs when σ belongs to the region between the curves $\sigma = \sigma_p$ and $\sigma = \theta\sigma_p$ or when (α, σ) belong to the region between the curves $\sigma = \sigma_{hP}(\alpha)$ and $\sigma = \sigma_{\theta hP}(\alpha)$, represented in Figure 9.

In fact, the curves denoted by $\sigma = \sigma_p$, $\sigma = \theta\sigma_p$, $\sigma = \sigma_{hP}$ and $\sigma = \sigma_{\theta hP}$ are no longer curves of pitchfork bifurcation or of Hopf bifurcation because the changes occur only in one of the Jacobian matrices associated with P, and it is not clear what is their effect on the dynamical behavior near the fixed point P. As we shall see in the next section, where some numerical examples are shown, if the parameters are taken in the region between the curves $\sigma = \sigma_p$ and $\sigma = \theta\sigma_p$, the fixed point P cannot be considered an attractor in the topological Lyapunov sense: we remark that such definition ensures that the system remains close to the equilibrium for arbitrary small perturbations in any direction.

The region between the two curves $\sigma = \sigma_{hP}$ and $\sigma = \sigma_{\theta hP}$ is particular. In those regimes the Hopf theorem cannot be applied. However, the spiralling character of the trajectories, due to the complex eigenvalues, can lead to the conclusion that an attracting set may exist anyway. These particular cases will be better analyzed through the numerical explorations discussed in the next section

6 Global dynamics of the map $\widetilde{T}$

In this section, by the same "modus operandi" as in Section 4, we note some numerical results obtained by following some particular bifurcation paths in the space of the parameters. In order to compare the new situations with those obtained for the symmetric model, we consider fixed values of some parameters, namely $\theta = 1.2$, $\delta = 0.2$, $\gamma = 0.6$. For this set of parameters we have $\sigma_p = 0.25$ and $\theta\sigma_p = 0.3$. We first consider $\alpha = 0.9$, and we increase the parameter σ from 0 to 1.

For $\sigma < \sigma_p$ the map $\widetilde{T}$ has two stable fixed points R and Q, and the fixed point P is a kind of saddle point, the stable set of which separates the basins of attraction $\mathscr{B}(R)$ and $\mathscr{B}(Q)$ (see Fig. 10a, obtained for $\sigma = 0.2$). In fact, for $0 < \sigma < \sigma_p$, P is a saddle both for the matrix $DT(P)$ and $DT_\theta(P)$.

As σ increases approaching σ_p , the fixed point Q approaches P, and at $\sigma = \sigma_p$ the fixed point Q merges with P, so that for $\sigma > \sigma_p$ only the fixed points R and P exist. For $\sigma_p < \sigma < \theta\sigma_p$ R is a stable node and P is not attracting from a topological point of view, since it is a stable node for the matrix $DT(P)$, whereas it is a saddle point for the matrix $DT_\theta(P)$. This situation is represented in Figure 10b, obtained for $\sigma = 0.26$. The light grey region is the basin of the stable fixed point R, and the white region represents the set of points the trajectories of which converge to P; however, the fixed point P belongs to the boundary of its "basin" and consequently it is not stable with respect to arbitrarily small perturbations to the left of P.
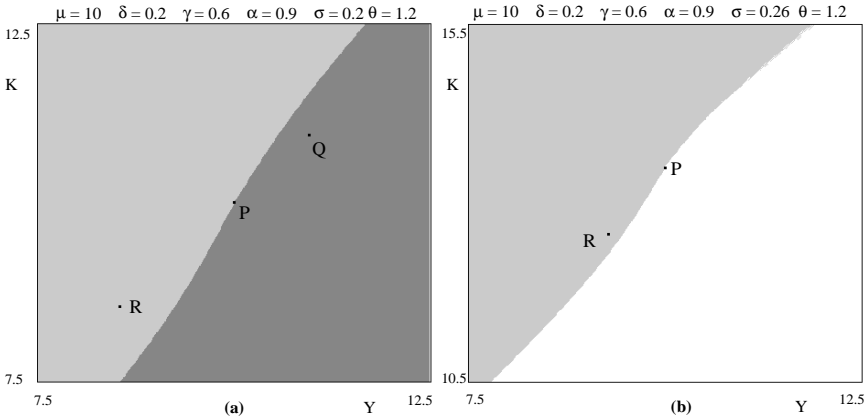
Fig. 10 a,b. Non-symmetric model with $\theta = 1.2$. **a** For $\mu = 10$, $\delta = 0.2$, $\gamma = 0.6$ $\alpha = 0.9$ and $\sigma = 0.2$, i.e. $\sigma < \sigma_p$, three fixed points of the map $\widetilde{T}$ exist: P is a saddle point (for both the jacobian matrices $DT(P)$ and $DT_\theta(P)$), R and Q are stable foci. The stable set of P constitutes the boundary that separates the basins $\mathscr{B}(R)$ and $\mathscr{B}(Q)$, represented by light grey and dark grey regions respectively. **b** For $\sigma = 0.26$, $\sigma_p < \sigma < \theta\sigma_p$, only the two fixed points R and P exist. R is stable (stable focus) and P is not stable in the classical sense, although it attracts the points in the white region. However, from a practical point of view (and also for numerical experiments, due to the presence of round-off errors), the points belonging to the white regions eventually reach the equilibrium R, since small perturbations cause such trajectories to move far from P

As σ approaches $\theta\sigma_p$ the stable fixed point R approaches P and merges into it at $\sigma = \theta\sigma_p$. Then, for $\sigma > \theta\sigma_p$, P is a topological attractor with a large basin (numerically it seems to attract all the points of the phase plane). The sequence of bifurcations described above is summarized, as a function of σ, in the bifurcation diagram shown in Figure 11.

Another interesting sequence of local and global bifurcations is observed if we consider the path with $\alpha = 1.15$ and σ increasing from 0 to 1. This path crosses the bifurcation curves $\sigma = \sigma_p$ and $\sigma = \theta\sigma_p$ in a regime in which the fixed point P is unstable (with respect to both the Jacobian matrices $DT(P)$ and $DT_\theta(P)$).
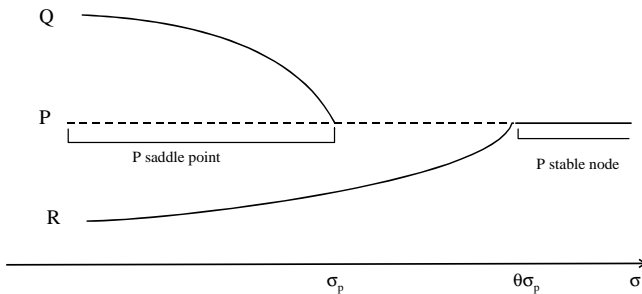
Fig. 11. Bifurcation diagram that qualitatively represents the dynamic scenarios and the bifurcations that are met for the non-symmetric model along the path with fixed $\alpha = 0.9$ and σ varying in the range $(0, 1)$
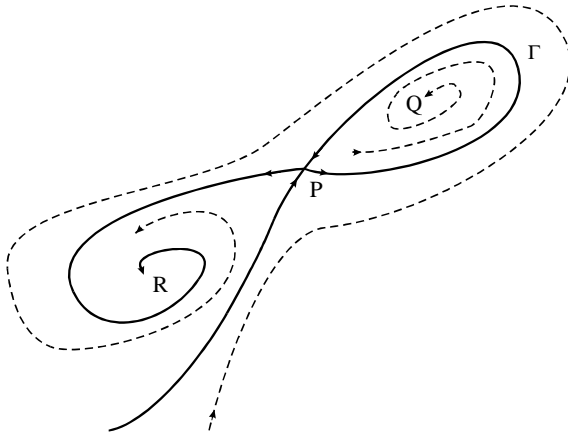
Fig. 12. Qualitative sketch of the dynamic scenario at the global bifurcation value $\sigma = \sigma_{gQ}$. The homoclinic loop around Q is repelling both from inside and outside
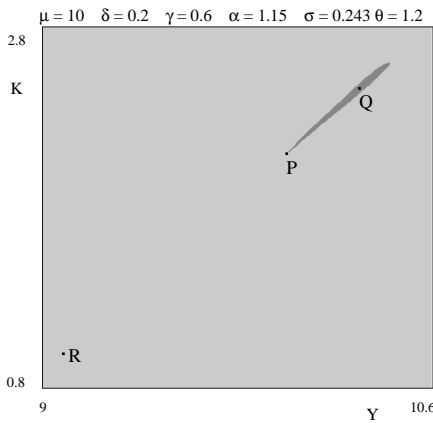
Fig. 13. For $\alpha = 1.15$ and $\sigma = 0.243$, i.e. just after the bifurcation at $\sigma = \sigma_{gQ}$, two stable equilibria exist, R and Q, with respective basins $\mathcal{B}(R)$ and $\mathcal{B}(Q)$, represented by light grey and dark grey regions respectively

At $\sigma = 0.23 < \sigma_p$ the map $\widetilde{T}$ has two stable fixed points, R and Q and an unstable fixed point P, of saddle type, the stable set of which constitutes the boundary that separates the two basins $\mathcal{B}(R)$ and $\mathcal{B}(Q)$ (a situation similar to the one shown in Fig. 10a). As σ increases, a global bifurcation (at a value $\sigma_{gQ} < \sigma_p$) occurs associated with the map T: the stable and unstable "branches" of P associated with the Jacobian $DT(P)$ merge, forming a loop in P, i.e. a homoclinic orbit Γ, as qualitatively shown in Figure 12. We note that the homoclinic orbit Γ is unstable, both inside and outside. This homoclinic orbit disappears for $\sigma > \sigma_{gQ}$, leaving a repelling closed invariant curve Γ_Q in the half-plane $Y > \mu$, which is the boundary of the basin of attraction $\mathcal{B}(Q)$ of the fixed point Q (see Figure 13, obtained for $\sigma = 0.243$). Thus, this global bifurcation has the effect

of an enlargement of the basin $\mathscr{B}(R)$, since it now covers a much larger portion of the phase space, around the other stable fixed point Q.

As σ increases, another global bifurcation occurs at a value $\sigma = \sigma_{hQ}$. In fact, as σ increases, the invariant curve Γ_Q shrinks into Q in a subcritical Hopf bifurcation, transforming Q into a repelling focus. Then Q approaches P and, at $\sigma = \sigma_p$, Q merges with P and disappears.

For $\sigma > \sigma_p$, in the interval $\sigma_p < \sigma < \theta\sigma_p$, another global bifurcation will occur at $\sigma = \sigma_{gR}$, which is again a homoclinic bifurcation of P but associated with the map T_θ, being due to the merging of the stable and unstable "branches" of P associated with the Jacobian $DT_\theta(P)$.
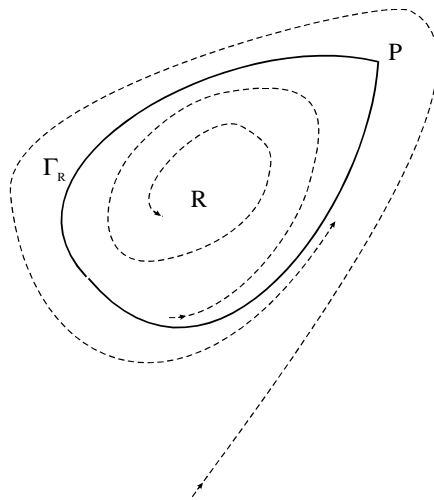
Fig. 14. Qualitative sketch of the homoclinic loop at the bifurcation value $\sigma = \sigma_{gR}$. The homoclinic loop around R is repelling from inside and attracting from outside

This homoclinic connection generates a closed invariant curve Γ_R which, *differently from the previous global bifurcation occurring at σ_{gQ}, is attracting from the outside, repelling inside* (see the qualitative sketch in Fig. 14). This means that Γ_R is given by the "merging" of two invariant closed curves which shall split after the bifurcation. In fact, for $\sigma > \sigma_{gR}$, we observe a closed invariant curve Γ, which attracts the widest portion of points in the phase plane, and a repelling closed invariant curve Γ_R focus), as shown in Figure 15, obtained for $\sigma = 0.2715$. As expected, as σ is further increased, the basin $\mathscr{B}(R)$ becomes smaller and smaller and Γ_R shrinks into R in a subcritical Hopf bifurcation leaving a repelling focus R, which will become a repelling node, approaching P for increasing values of σ and then merging with it at $\sigma = \theta\sigma_p$. After this, the only attractor will be the closed invariant curve Γ (which seems to attract all the points of the plane). This closed invariant curve Γ persists, decreasing in size and approaching P: as we have numerically observed, a closed invariant attracting curve Γ still persists in the interval $\sigma_{hP} < \sigma < \sigma_{\theta hP}$ (see the bifurcation
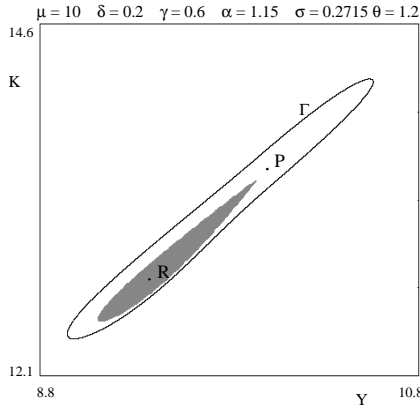
Fig. 15. For $\alpha = 1.15$ and $\sigma = 0.2715$, i.e. just after the bifurcation at $\sigma = \sigma_{gR}$, there are two fixed points, R and P, stable and unstable, respectively. The basin $\mathcal{B}(R)$ is represented by the grey region, whereas the points of the white region generate trajectories converging to the limit cycle Γ that surrounds both the equilibria
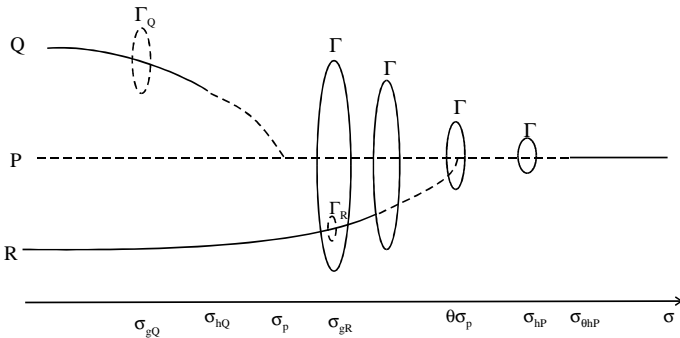
Fig. 16. Bifurcation diagram that qualitatively represents the dynamic scenarios and the bifurcations that are met for the non-symmetric model along the path with fixed $\alpha = 1.15$ and σ varying in the range $(0, 1)$

diagram of Fig. 16); it shrinks around P and then merges with it at $\sigma = \sigma_{\theta h P}$, after which P becomes an attracting fixed point.

The sequence of dynamic scenarios described above are schematically represented in the bifurcation diagram of Figure 16.

7 Conclusions

The version of the Kaldor business-cycle model analyzed in this paper allowed us to obtain some new dynamic scenarios which may be interesting both for the applied dynamicist and the economist. From the point of view of the mathematical methods, the interest lies in the fact that the main results are obtained through a study of global bifurcations, in particular homoclinic bifurcations, the study of which often requires a continuous interplay among analytic, geometric

and numerical methods (and our analysis confirms this). Our contribution proves, thanks to a deeper analysis of the global dynamic properties of the Kaldor model, the existence of stable oscillations in the more realistic parameter constellations characterized by low values of the propensity to save, where three steady states exist. Such oscillations occur along an attracting limit cycle, surrounding the three steady states, which is created through a global (homoclinic) bifurcation. This leads to a situation of multistability, characterized by the presence of three coexisting attractors: two stable steady states and a stable limit cycle around them, each with its own basin of attraction. This occurs for parameter ranges that are slightly different with respect to the ones usually proposed in the literature on discrete-time versions of the Kaldor model, where the analysis is usually concerned with the creation of complex attractors around the unique (unstable) equilibrium, observed for very high values of the adjustment parameter α and sufficiently high values of the propensity to save σ. Instead, we focused our attention on the dynamic situations occurring for relatively low (and more realistic) values of the parameters σ and α, for which three steady state exist.

It is important to notice some analogies and differences between the model analyzed here and the one proposed by Kaldor (1940). Kaldor refers to the existence of three steady states, but such equilibria emerge only under the preliminary assumption that the capital stock is fixed. In other words, Kaldor builds up his dynamic analysis by assuming that, as in the standard Keynesian model, investment only constitutes, at a first stage, a component of demand, and only later contributes to the variation of the capital stock. More precisely, the dynamics in the Kaldor paper is composed of two steps: in the first (short run), Kaldor assumes that the capital stock is given and compares the propensity to save and the propensity to invest; in the second (long run) Kaldor analyzes the shifts of the saving and investment functions due to the endogenous changes in the capital stock caused by investment expenditure. In the model studied in this paper, as is usual in dynamic models, the investment at a given time period simultaneously influences the aggregate demand and the capital stock. This implies, among other things, that, while in the Kaldor model the two external steady states are unstable in the long run, this is not necessarily true in our dynamic model.

A second point is that the Kaldor model contributes to the Keynesian idea that expectations are to be considered as an exogenous factor. In fact, besides the difficulty introducing rational expectations into a model with three coexisting equilibria, we must also consider the uncertainty in the equilibrium selection induced by the possibility that the basins of attraction of the coexisting stable equilibria may be very intermingled (see Fig. 3). In such uncertain situations, the most natural assumption is that agents expect the "normal" output level. We notice that in the case of convergence to one of the two external equilibria, a modification of the "normal" (and expected) output level may be introduced, but this should cause a structural change of the model. In order to maintain our analysis inside the framework of dynamical systems, this possibility has not been considered in the present paper. However, we underline that the exogenous

nature of the "gravity center" of the economic system is a typical Keynesian and Kaldorian feature.

A third point worth noting concerns the role of propensity to save. Our results confirm that, at least in the short run, a high propensity to save has a stabilizing role. This suggests the possibility of inhibiting the onset of cyclic behaviors by controlling the agents' propensity to save through, for example, fiscal policies. We remark that also this result has an evident "Kaldorian flavor".

A Local stability

In this appendix, we analyze the local stability of the fixed points of the map T, given in (3), and $\widetilde{T}$, given in (9), in order to prove the statements concerning the stability of the fixed points given in the Propositions 1 and 2.

A.1 Map T

The study of the local stability of the fixed point $P = (\mu, \mu\frac{\sigma}{\delta})$ is obtained through the localization, on the complex plane, of the eigenvalues of the Jacobian matrix of T

$$DT(Y,K) = \begin{bmatrix} 1 + \frac{\alpha}{1+(Y-\mu)^2} - \alpha\sigma & -\alpha\gamma \\ \frac{1}{1+(Y-\mu)^2} & 1 - \delta - \gamma \end{bmatrix} \tag{12}$$

computed at the fixed point P:

$$DT(\mu, \mu\frac{\sigma}{\delta}) = \begin{bmatrix} 1 + \alpha(1-\sigma) & -\alpha\gamma \\ 1 & 1 - \delta - \gamma \end{bmatrix} \tag{13}$$

The eigenvalues of (13) are the solutions of the characteristic equation:

$$P(z) = z^2 - Tr\ z + Det = 0 , \tag{14}$$

where Tr and Det are, respectively, the trace and the determinant of (13):

$$Tr = 2 + \alpha(1-\sigma) - (\delta+\gamma) ;$$

$$Det = (1-\gamma-\delta)(1-\alpha\sigma) + \alpha(1-\delta).$$

A sufficient condition for the stability of a fixed point is expressed by the following system of inequalities

$$\begin{cases} P(1) = 1 - Tr + Det > 0 & \text{(a)} \\ P(-1) = 1 + Tr + Det > 0 & \text{(b)} \\ P(0) = Det < 1 & \text{(c)} \end{cases} . \tag{15}$$

that give necessary and sufficient conditions for the two roots of (14) to be inside the unit circle of the complex plane (see, for example, Gumowski and Mira, 1980, p. 159).

The inequality (15a) can be reformulated as

$$\sigma > \frac{\delta}{\delta + \gamma}$$

so that, whenever three fixed points exist, the central fixed point P cannot be stable.

The inequality (15b) becomes

$$\alpha(1 - \sigma)(2 - \delta) + \alpha\sigma\gamma + 2(2 - \gamma - \delta) > 0$$

and, being $0 < \delta < 1$, $0 < \sigma < 1$ and $\alpha > 0$, the condition (15b) is always verified provided that $\gamma < 2 - \delta$, which is satisfied if γ is assumed to vary in the range of its economically plausible values, i.e. $\gamma < 1$.

Condition (15c) becomes

$$\alpha\sigma(1 - \gamma - \delta) > \alpha(1 - \delta) - (\gamma + \delta) ,$$

which, for $\gamma + \delta < 1$, is equivalent to:

$$\sigma > \frac{1 - \delta}{1 - \gamma - \delta} - \frac{\gamma + \delta}{\alpha(1 - \gamma - \delta)} ,$$

and for $\gamma + \delta > 1$ to:

$$\sigma < -\frac{1 - \delta}{\delta + \gamma - 1} + \frac{\gamma + \delta}{\alpha(\delta + \gamma - 1)} .$$

For values of the parameters into their realistic ranges, the three conditions (15) are satisfied inside the region $ABCD$ represented in Figure 1. For $\sigma = \frac{\delta}{\delta+\gamma}$, on the lower boundary of the region $ABCD$, we have $P(1) = 0$, i.e. one root of (14) is on the boundary of the unit circle in the point $z = 1$, and for decreasing values of σ this root exits the unit circle, and two fixed points are created. This is a typical *pitchfork bifurcation* (see e.g. Guckenheimer and Holmes, 1983; or Lorenz, 1993)[8]. For $\sigma = \frac{1-\delta}{1-\gamma-\delta} - \frac{\gamma+\delta}{\alpha(1-\gamma-\delta)}$, on the right boundary of the region $ABCD$, we have $Det = 1$, i.e. two complex conjugate roots of (14) with modulus equal to 1, and if the parameters α and/or σ are varied so that the point (α, σ) crosses the portion CD of the hyperbola from left to right, the two eigenvalues exit the unit circle, and a Hopf bifurcation occurs (see e.g. Guckenheimer and Holmes, 1983; or Lorenz, 1993)[9].

---

[8] A *pitchfork bifurcation* of a fixed point is related to an eigenvalue which exits the unit circle through the value $z = 1$ and the simultaneous creation of two new fixed points along the invariant manifold associated with the bifurcating eigenvalue. It is *supercritical* if the two fixed points are stable along the invariant manifold, *subcritical* if the two fixed points are unstable and merge with the central stable fixed point at the bifurcation value.

[9] We recall that a Hopf bifurcation of a fixed point, related to a pair of complex conjugate eigenvalues which exit the unit circle, is called *supercritical* if an attracting closed invariant curve is created around the unstable fixed point. It is called *subcritical*, if a repelling closed invariant curve exists around the stable fixed point, and merges with it at the bifurcation value (see e.g. Guckenheimer and Holmes, 1983). A rigorous proof of the supercritical or subcritical nature of a Hopf bifurcation requires a center manifold reduction and the evaluation of higher order derivatives (up to the third order). In this case, the numerical detection of stable closed invariant curves around the unstable fixed point reveals the supercritical nature of the bifurcation.

In order to study the stability and local bifurcations of the fixed points R and Q, we compute the eigenvalues of the Jacobian matrix

$$DT(R) = DT(Q) = \begin{bmatrix} 1 + \frac{\alpha}{1+(Y_R-\mu)^2} - \alpha\sigma & -\alpha\gamma \\ \frac{1}{1+(Y_R-\mu)^2} & 1 - \delta - \gamma \end{bmatrix} \tag{16}$$

Unfortunately, Y_R cannot be computed analytically, so only a numerical evaluation of the eigenvalues is possible. However, the conditions (15) can still be analyzed, since they become, respectively,

$$\begin{cases} P(1) = \alpha \left(\sigma(\gamma+\delta) - \frac{\delta}{1+(Y_R-\mu)^2} \right) > 0 & \text{(a)} \\ P(-1) = \alpha(2-\delta)\left(\frac{1}{1+(Y_R-\mu)^2} - \sigma \right) + \alpha\sigma\gamma + 2(2-\gamma-\delta) > 0 & \text{(b)} \\ P(0) = (1-\gamma-\delta)(1-\alpha\sigma) + \frac{\alpha(1-\delta)}{1+(Y_R-\mu)^2} < 1 & \text{(c)} \end{cases} \quad .$$
$$\tag{17}$$

A.2 Map $\widetilde{T}$

The Jacobian matrix of the map $\widetilde{T}$ is defined as

$$D\widetilde{T}(Y,K) = \begin{cases} DT(Y,K) & \text{if } Y > \mu \\ DT_\theta(Y,K) & \text{if } Y < \mu \end{cases}, \tag{18}$$

where DT is the Jacobian matrix of the map T given in (12), and

$$DT_\theta(Y,K) = \begin{bmatrix} 1 + \frac{\theta\alpha}{1+(Y-\mu)^2} - \alpha\sigma & -\alpha\gamma \\ \frac{\theta}{1+(Y-\mu)^2} & -(\delta+\gamma-1) \end{bmatrix}. \tag{19}$$

So, the local behavior on the right of $P = (\mu, \mu\frac{\sigma}{\delta})$ is governed by the Jacobian matrix (13), whereas the local behavior on the left of P is governed by the Jacobian matrix:

$$DT_\theta(P) = \begin{bmatrix} 1 + \alpha(\theta-\sigma) & -\alpha\gamma \\ \theta & -(\delta+\gamma-1) \end{bmatrix}.$$

The analysis of the eigenvalues of $DT(P)$ is considered in A.1; by considering, in a similar way, the general stability conditions (15) for the matrix $DT_\theta(P)$, we can conclude that the eigenvalues of the matrix $DT_\theta(P)$ are inside the unit circle in the complex plane if and only if the following inequalities hold:

$$\sigma > \theta\sigma_p = \theta\frac{\delta}{\delta+\gamma};$$

and

$$\sigma > \sigma_{\theta hP}(\alpha) = \frac{\theta(1-\delta)}{1-\gamma-\delta} - \frac{\gamma+\delta}{\alpha(1-\gamma-\delta)} \qquad \text{if } (\gamma+\delta) < 1$$

or $\qquad \sigma < \sigma_{\theta hP}(\alpha) = -\frac{\theta(1-\delta)}{\delta+\gamma-1} + \frac{\gamma+\delta}{\alpha(\delta+\gamma-1)} \qquad \text{if } (\gamma+\delta) > 1 \ .$

B Symmetry properties of the map T

The map T is symmetric with respect to the fixed point $P = (\mu, \mu\frac{\sigma}{\delta})$. This means that symmetric points are mapped into symmetric points (with respect to P). Denote by $F_1(Y, K)$ and $F_2(Y, K)$ the two components of the map T:

$$F_1(Y, K) = Y + \alpha\sigma\mu + \alpha\gamma\left(\frac{\sigma\mu}{\delta} - K\right) + \alpha\arctan(Y - \mu) - \alpha\sigma Y$$
$$F_2(Y, K) = \sigma\mu + \gamma\left(\frac{\sigma\mu}{\delta} - K\right) + \arctan(Y - \mu) + (1 - \delta)K$$

and observe that the symmetric of the point (Y, K) with respect to P is the point $(2\mu - Y, 2\frac{\sigma\mu}{\delta} - K)$. The above property, which can easily be verified, can be formalized as follows:

$$F_1(2\mu - Y, 2\frac{\sigma\mu}{\delta} - K) = 2\mu - F_1(Y, K)$$
$$F_2(2\mu - Y, 2\frac{\sigma\mu}{\delta} - K) = 2\frac{\sigma\mu}{\delta} - F_2(Y, K)$$

This implies that a cycle of T is either symmetric with respect to P or admits a symmetric cycle (in particular, the equilibria Q and R are located in symmetric position with respect to P).

References

Abraham R, Shaw CD (1992) Dynamics, the geometry of behaviour. Addison Wesley, New York

Abraham R, Gardini L, Mira C (1997) Chaos in discrete dynamical systems (a visual introduction in two dimensions). Springer, Berlin Heidelberg New York

Bischi GI, Gardini L, Kopel M (2000) Analysis of Global bifurcations in a market share attraction model. Journal of Economic Dynamics and Control 24: 855–879

Brock WA, Hommes CH (1997) A rational route to randomness. Econometrica 65: 1059–1095

Chang WW, Smith DJ,(1971) The Existence and persistence of cycles in a non-linear model: Kaldor's 1940 model re-examined. Review of Economic Studies 38: 37–44

Dana RA, Malgrange P (1984) The Dynamics of a discrete version of a growth cycle model. In: J.P. Ancot (ed.) Analysing the structure of economic models pp 205–222. Martinus Nijhoff, The Hague

Gabisch G, Lorenz HW (1989) Business cycle theory , 2nd ed. Springer, Berlin Heidelberg New York

Gardini L (1993) On a model of financial crisis: critical curves as a new tool of global analysis. In: Gori F, Galeotti M (eds.) Nonlinear dynamics in economics and social sciences, pp 252–263. Springer, Berlin Heidelberg New York

Grasman J, Wentzel JJ (1994) Co-existence of a limit cycle and an equilibrium in a Kaldor's business cycle model and its consequences. Journal of Economic Behavior and Organization 24: 369–377

Guckenheimer J, Holmes P (1983) Nonlinear oscillations, dynamical systems, and bifurcations of vector fields. Springer, Berlin Heidelberg New York

Gumowski I, Mira C (1980) Dynamique chaotique. Cepadues Ed. Toulouse

Herrmann R (1985) Stability and chaos in a kaldor-type model. DP22, Department of Economics, University of Göttingen

Kaldor N (1940) A model of the Trade Cycle. Economic Journal 50:78–92; reprinted in (1964) Essays on economic stability and growth, 177–192 Duckworth, London

Lorenz HW (1992)Multiple attractors, complex basin boundaries, and transient motion in deterministic economic systems. In Feichtinger G (ed.) Dynamic Economic Models and Optimal Control pp.411–430. North-Holland, Amsterdam

Lorenz HW (1993) Nonlinear Dynamical economics and chaotic motion, 2nd ed. Springer, Berlin Heidelberg New York

Mira C, Gardini L, Barugola A, Cathala JC, (1996) Chaotic dynamics in two-dimensional noninvertible maps. World Scientific, Singapore

Palis J, Takens F (1993) Hyperbolicity and sensitive chaotic dynamics at homoclinic bifurcations. Cambridge University Press, Cambridge

Rodano G (1997) Lezioni sulle teorie della crescita e sulle teorie del ciclo. Dipartimento di Teoria Economica e Metodi Quantitativi, Università di Roma "La Sapienza"